Nonholonomic Robot Navigation of Mazes using Reinforcement Learning

Daniel Gleason[a] and Michael Jenkin[b]
Electrical Engineering and Computer Science,
Lassonde School of Engineering, York University, Toronto, Canada

Keywords: Robot Navigation, Reinforcement Learning, Navigating Mazes.

Abstract: Developing a navigation function for an unknown environment is a difficult task, made even more challenging when the environment has complex structure and the robot imposes nonholonomic constraints on the problem. Here we pose the problem of navigating an unknown environment as a reinforcement learning task for an Ackermann vehicle. We model environmental complexity using a standard characterization of mazes, and we show that training on complex maze architectures with loops (braid and partial braid mazes) results in an effective policy, but that for a more efficient policy, training on mazes without loops (perfect mazes) is to be preferred. Experimental results obtained in simulation are validated on a real robot operating both indoors and outdoors, assuming good localization and a 2D LIDAR to recover the local structure of the environment.

1 INTRODUCTION

There has been considerable success in applying deep Reinforcement Learning (DRL) to robot navigation both with (Faust et al., 2018) and without (Tai et al., 2017; Devo et al., 2020; Wanmg et al., 2021) a map. One concern with a number of existing DRL-based approaches to the navigation problem is the nonholonomic nature of most autonomous vehicles. DRL-based approaches typically assume either holonomic motion or differential drive vehicles with separately controllable linear and angular velocity. How well do DRL-based approaches function when strong nonholonomic motion constraints are considered, and how is performance impacted when environments of different complexity are considered for both training and evaluation? To address these concerns, here we consider the application of End-to-End Reinforcement Learning (E2E-RL) (Tai et al., 2017) to obtain a navigation function for an Ackermann vehicle for environments of different complexities, and compare performance against a random action baseline and a baseline based on Hierarchical Reinforcement Learning (HRL) (Faust et al., 2018) exploiting waypoints obtained using a sample-based planning algorithm (RRT*) (Karaman and Frazzoli, 2011). DRL-based navigation functions are constructed through learning on environments of different complexities and these navigation functions are evaluated on environments of different complexity as well.

The main contributions of this paper are:

- We demonstrate that DRL can be used to provide effective navigation control for a nonholonomic vehicle operating in a maze-like environment.
- We demonstrate that training on different environmental complexity classes impacts vehicle performance, with training on more complex environments – particularly environments with loops – resulting in more robust navigation while training on simpler environments – environments without loops – resulting in more efficient navigation.

The remainder of this paper is structured as follows. Section 2 describes previous work in DRL-based navigation, on sampling-based path planning, and on the classification of maze complexity. Section 3 describes the formulation of maze navigation using DRL used in this work. Section 4 describes experimental results and with a skid-steer robot simulating a vehicle using Ackermann steering in both indoor and outdoor environments. Finally, Section 5 summarizes the work and provides suggestions for future work.

[a] https://orcid.org/0000-0003-0816-5689
[b] https://orcid.org/0000-0002-2969-0012

Gleason, D. and Jenkin, M.
Nonholonomic Robot Navigation of Mazes using Reinforcement Learning.
DOI: 10.5220/0011123600003271
In *Proceedings of the 19th International Conference on Informatics in Control, Automation and Robotics (ICINCO 2022)*, pages 369-376
ISBN: 978-989-758-585-2; ISSN: 2184-2809

2 PREVIOUS WORK

2.1 Deep RL for Continuous Action Spaces

Reinforcement Learning (RL) is a category of Machine Learning where the goal is to train a software agent to take actions in an environment which maximizes the cumulative reward it receives. Deep Reinforcement Learning (DRL) has been successfully applied to a wide range of difficult problems, such as Atari games (Mnih et al., 2013), Go (Silver et al., 2016), and 3D locomotion (Schulman et al., 2015). DRL has also been shown to work well for both map and mapless robot navigation with continuous control (Faust et al., 2018; Tai et al., 2017).

In RL and DRL the task is modelled as a Markov Decision Process (MDP). At each time step, the agent observes the state of the environment, s_t, then takes an action, a_t. Based on this state-action pair, (s_t, a_t), the agent receives a reward, r_t, and the agent transitions to the next state, s_{t+1}. The way in which the agent chooses its actions is called the policy and is denoted as π. Specifically, the policy defines the probability of taking a possible action given the current state, written as $\pi(a_t|s_t)$.

The agent's goal is to find the policy which maximizes its cumulative reward. Reinforcement Learning (RL) methods can be broadly defined as being either Policy-based or Value-based. Policy-based methods aim to learn the optimal policy directly, while Value-based methods aim to learn the value of each action in a given state, meaning that the optimal policy is to choose the action with the highest value. Actor-Critic methods (Mnih et al., 2016) are a category of Reinforcement Learning methods which combine Policy-based and Value-based learning. The Actor learns the policy directly while the Critic learns a value function to use to reduce the variance when training the Actor. Soft Actor-Critic (SAC) is an off-policy, Actor-Critic algorithm which incorporates entropy regularization (Haarnoja et al., 2018). In this work we use Soft Actor-Critic (SAC) algorithm (Haarnoja et al., 2018) as it has been shown to be an effective deep RL algorithm for continuous action spaces.

2.2 Deep RL for Mapless Navigation

Tai et al. (2017) use End-to-end deep Reinforcement Learning to solve mapless navigation for a differential drive robot. The robot is able to generalize to unseen environments and transfer a policy learned in simulation to real-world environments with no additional training. They use sparse range findings from a LIDAR for obstacle detection so as to reduce the gap between simulation and the real world. The output action of their RL algorithm is the linear and angular velocities the robot should use to move. For their deep RL algorithm they used Asyncronous Actor-Critc (A3C) (Mnih et al., 2016). The work reported here is motivated by the approach described in Tai et al. (2017).

2.3 Sample-based Path Planning

Sample-based path planning methods use random sampling of the environment to overcome the computational cost of complete planning algorithms (Dudek and Jenkin, 2000). While not all sample-based methods are guaranteed to find an optimal path, like a search of the entire configuration space would, they can often find a valid path much more quickly(Dudek and Jenkin, 2000). Here we use RRT* (Karaman and Frazzoli, 2011), an optimized version of the Rapidly Exploring Random Tree (RRT) algorithm (Lavalle, 1998) as an informed baseline to evaluate a DRL-based navigation function. We perform local path following using a DRL-based path following process to deal with the constraints introduced by Ackermann steering. We refer to this approach as hierarchical reinforcement learning (HRL). HRL provides a baseline that separates the problem of path following from path execution but which still meets the requirements of Ackermann-based steering.

2.4 Types of Mazes

Mazes and labyrinths have a long history (see Matthews, 1972, for a review). Although the terms maze and labyrinth are often used interchangeably, the terms are traditionally used to define different structures. The term maze refers to a complex branching path structure while the term labyrinth refers to a single-path structure with no branching paths. There exists a standard taxonomy of maze subgroups (Pullen, 2020). Of particular interest in this work are labyrinths and the perfect maze, braid maze, and partial-braid maze subgroups. For the labyrinth and each of the maze types we identify two specially marked locations, a start location, and a single goal location. In terms of the environment structure: A labyrinth is a maze with only one path. The agent can move from the start to the goal without having to make any decisions about which path to take. A perfect maze has no loops and can be described as a tree of labyrinths.A braid maze is a maze without any dead ends, which can be thought of as a labyrinth with loops. A partial-braid maze is a braid maze with

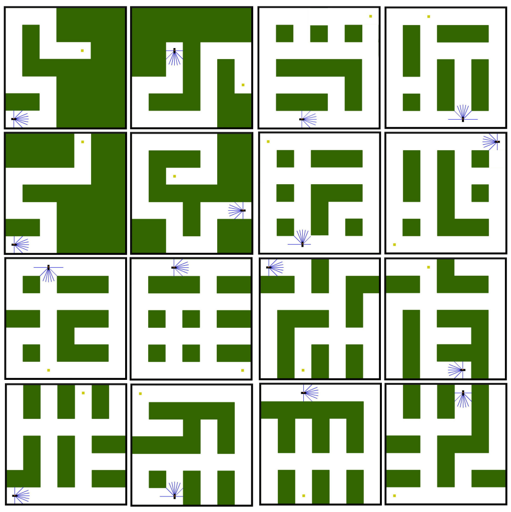
Figure 1: Sample 7x7 mazes. The upper left quadrant shows four labyrinths, the upper right four braid mazes, the lower left four partial braid mazes and the lower right four perfect mazes. The robot is simulated in each maze along with its simulated LIDAR shown as a collection of blue rays. The robot's position is at the intersection of these rays. The robot's goal location is identified by a dot.

dead ends, which is the most difficult type of maze to solve. Figure 1 provides examples of 7x7 maze environments from these groups.

3 MAZE NAVIGATION USING DRL AND HRL

In Tai et al. (2017) , RL-based path planning is considered in the context of a differential drive vehicle operating under the assumption that the vehicle has independent control of its linear and angular velocity. Such a policy is not possible for an Ackermann drive vehicle in which changes in position and orientation are more tightly linked. This constraint limits the paths that the robot can take and makes the navigation and path planning tasks more complex.

The RL component of the local planning for HRL and the end-to-end planning for E2E-RL is defined by three aspects: the state space, the action space, and the reward function, as described below:

State Space. The state space includes obstacle range findings and the orientation of the robot. The obstacle range information models a LIDAR sampling nine equally spaced orientations from $-\pi/2$ to $\pi/2$ radians about zero, the straight ahead direction. For the HRL approach only, the state space includes the next n way points along the path, provided by RRT*, as the x and y displacements from the vehicle's current position to the way points. If there are less than n points left in the path, the last point (the goal) is repeated to ensure there are n points in the state. E2E-RL is only provided with the x and y displacement to the goal point. All of these values are normalized as follows: the range findings by dividing the observed distance by the maximum distance, the orientation by dividing by 2π, and the x and y distances by dividing by the environment width and length respectively.

Action Space. The robot's linear velocity V is set to a constant, meaning the vehicle always moves forward. The RL agent controls the steering amount. The steering amount is a value between -1 and 1, corresponding to a change in the vehicle's steering angle equal to: $(V\theta)/(L*C)$. Where V is the vehicle's velocity, L is the vehicle's length, C is a constant to control the minimum turning radius of tairpe vehicle, and θ is the steering amount. We selected a value of C which corresponded to a minimum turning radius approximately equal to the length of the robot.

Reward Function. The reward function is similar for both HRL and E2E-RL, with a slight addition to HRL to incorporate a reward for following the path. There is a max and min reward. Both approaches receive the max reward if they reach the goal and the min reward if they hit an obstacle, with both of these events terminating the episode. Otherwise, both receive an intermediary reward:

$$-\frac{1}{|R|}\sum_{r\in R}(1-r)^2$$

Where R is the set of range finding rays and r is a particular ray's normalized distance value. This rewards the RL agent for staying away from obstacles. The reward is framed as minimizing a negative function to incentivize the agent to end the episode as quickly as possible. Given that some of the environments contain loops, if this intermediary reward were positive the agent would be more likely to drive in a loop until the episode ends than attempt to reach the goal.

HRL receives an additional intermediary reward when it reaches a certain distance ε from the next point in the path. This reward is equal to the max reward divided by a constant K. When this occurs, the point is removed from the path and the next n points in the state are updated. The ε term controls how closely the path must be followed by the agent. Since for HRL the robot has the constraints of Ackermann steering but we are using straight-line connections for the points, ε must be sufficiently large to allow for the necessary deviations from the path.

4 EXPERIMENTAL RESULTS

4.1 Maze Generation

Python-Maze (Turidus, 2017) is used to generate the braid, partial-braid, and perfect mazes. These mazes are generated by selecting random start and goal blocks, with the condition that one must be on the top row and the other on the bottom. Then a perfect maze is generated between the selected start and goal. For braid and partial-braid, Python-Maze has an option which adds a percentage of loops to the maze, which was set to 100% for braid and 25% for partial-braid mazes.

Labyrinths are generated using a custom script. We randomly select start and goal blocks anywhere in the grid, with the only condition being that the euclidean distance between the two blocks be greater than a minimum distance Min. Min was set to 4 for the 7x7 mazes and 5 for the 9x9 mazes. Once the start and goal are selected, the algorithm randomly walks through the maze by blocks of two, starting at the start block, removing the walls it passed through. As we are generating labyrinths, the algorithm is not allowed to walk through blocks which had already been visited. The algorithm runs until it reaches the goal or gets stuck. If it gets stuck the algorithm is restarted. This process is repeated until a labyrinth is created that connects the start and goal blocks.

In order to provide an equitable comparison between the various maze classes (including labyrinth), we embed the maze structure on a rectangular grid in which one grid square is approximately 3 times the length of the vehicle and we assume that the minimum turning radius of the vehicle is approximately equal to the vehicle's length. The minimum obstacle is a square with a side length of approximately three times the length of the vehicle. Obstacles fill in an entire block in the underlying representation. See Figure 1 for examples.

4.2 Hyperparameters

Both HRL and E2E-RL were trained using the Stable Baselines (Hill et al., 2018) RL baselines. If not mentioned, the default hyperparameters were used. Both HRL and E2E-RL were trained using the SAC (Haarnoja et al., 2018) algorithm with a network architecture of 3 layers of size 512. This network architecture was used for the policy, value function, and both Q-value functions. Training was performed on mazes and labyrinths of size 7x7. Evaluation was performed on mazes and labyrinths of size 7x7 and 9x9.

The best model during training was selected by evaluating the current policy every K timesteps for M episodes, using a deterministic version of the policy, and saving the policy with the highest average reward across the evaluation episodes.

4.2.1 HRL

For the HRL approach, we trained for 1m timesteps with a replay buffer of 1m timesteps, which took approximately 10 hours. The policy was evaluated every 30k timesteps for 20 episodes. The episode length was 1.5k timesteps.

4.2.2 E2E-RL

For the E2E-RL approach, we trained for 2m timesteps with a replay buffer of 2m timesteps, which took approximately 20 hours. The time varied slightly depending on the maze type, as ones with more walls took longer due to the increase in the number of collision checks per timestep. The policy was evaluated every 45k timesteps for 205 episodes. The episode length was 4.5k timesteps. We trained for longer on E2E-RL because it took longer for the agent to learn, likely due to the increased challenge of the task. We used a longer episode length as the agent was not following an optimal path and thus could take longer to reach the goal.

4.3 Simulation

In order to better understand the performance of the path planning performance of RL, we compare performance against a baseline HRL approach similar to Faust et al. (2018) in which RRT* is used to solve the path planning task and RL is used to execute the identified path subject to the constraints of Ackermann steering. Evaluation is performed in simulation using randomly generated environments from the labyrinth, braid, partial-braid and perfect maze types. A random action policy baseline is also reported.

4.3.1 HRL Baseline

For the HRL baseline we trained on braid mazes and tested on all four mazes classes (Table 1). Since the agent is following a path obtained using RRT* for all mazes, we developed a single baseline. As shown in Table 1, training on braid mazes is sufficient for at least 95% success on braid, partial-braid, and perfect mazes. The agent's performance dropped on labyrinths, possibly due to the fact that in a labyrinth there was slightly less space to maneuver at each turn, given that in a labyrinth three of the four sides are walls, whereas in the other maze types, there are at

Table 1: HRL baseline successes out of 100 trails on 7x7 mazes.

Test → Train ↓	Laby-rinth	Braid	Partial Braid	Perfect
Braid	78	95	96	96

least two openings at each turning section. (See Figure 1 for examples of this.) The presence of two or more empty squares allows the agent to execute a wider turning arc.

The primary purpose of the HRL-baseline was to demonstrate that with sufficient map information, the RL approach was capable of overcoming the restrictions imposed by Ackermann steering given the tight confines of the environments being used.

4.3.2 Random Action Baseline

Given the start and goal locations, the random search randomly selects adjacent squares which are not blocked by an obstacle to move to, with the only condition being that it cannot travel to its previous square. This mimics the behaviour of our Ackermann simulations, which cannot move backwards. This prevents the random policy from turning into walls "accidentally", but the random policy will fail if it enters a dead end. The random baseline does not enforce Ackermann constraints on the motion of the vehicle. The algorithm is run until it reaches the goal square, crashes at a dead end, or exceeds a maximum number of steps. Figure 2 shows the probability of success of the algorithm on a given maze type after a given number of steps. Each data point was gathered by running the algorithm on 100 mazes of the given class. For labyrinth and braid mazes in which there are no dead ends, the algorithm can only fail by exceeding the maximum steps, the probability of success will eventually equal 1. Given the impossibility of failure, we do not report the random policy's performance in Tables 2 or 3.

For both the random baseline and E2E-RL, on perfect mazes we assume that the first step taken does not strike a wall. The reference angle of the robot is set in E2E-RL before we run it, and we select an angle that gives the agent a chance to reach the goal. Therefore we give the same benefit to the random search for the sake of a fair comparison.

4.3.3 E2E-RL

We investigate the performance of E2E-RL on evaluation sets of size 100 on 7x7 mazes (Tables 2 and 4), which is the size they were trained on, and on 100 mazes of size 9x9 (Table 3, 5) which represents a more complex maze than the training set.

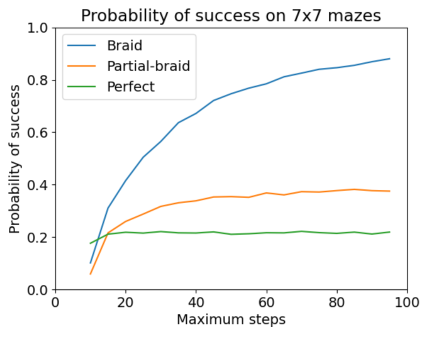

(a) 7x7 mazes

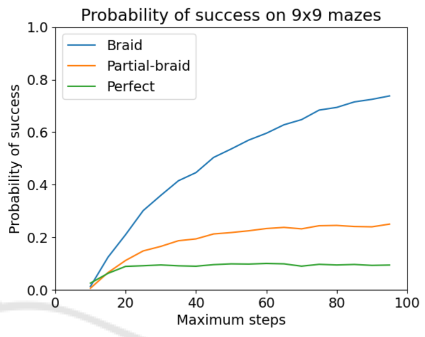

(b) 9x9 mazes

Figure 2: Probability of success for random baseline on different maze sizes. Each data point represents running the algorithm on 100 mazes.

The E2E-RL agents trained on partial-braid and perfect mazes significantly outperform the random search policy on mazes with dead ends (partial braid and perfect mazes). Interestingly, the agent trained on braid mazes did not outperform a random search on partial-braid mazes. This may be because the lack of dead ends in braid mazes led the agent to focus on learning optimal local path execution rather than optimal global navigation. This is supported by the fact that the braid maze agent outperformed all the agents on the labyrinth mazes, even the labyrinth agent itself.

For both 7x7 and 9x9 mazes the agent trained on labyrinths performed well on labyrinths and poorly on the rest. This was expected as this agent had no need to learn any global navigation behaviour and could focus solely on local path execution. For 7x7 mazes it is interesting that the agent trained on braid mazes outperformed the labyrinth agent on its own maze type. A potential reason for this is that the braid agent was exposed to more variety in training due to the numerous paths available given the loops, while the labyrinth agent was exposed to more simple structures during training. Perhaps the most striking result is that the partial braid agent performs very well (the best or very close to the best) on all classes on the 9x9 maze evaluation. Again, this may be the result of

Table 2: E2E-RL successes out of 100 trails on 7x7 mazes. Best performing policy is in bold.

Test → Train ↓	Laby-rinth	Braid	Partial Braid	Perfect
Labyrinth	94	34	23	20
Braid	**96**	64	35	32
Partial Braid	83	**80**	**64**	49
Perfect	68	78	62	**51**
Random	-	-	37	22

Table 3: E2E-RL successes out of 100 trails on 9x9 mazes. Best performing policy is in bold.

Test → Train ↓	Laby-rinth	Braid	Partial Braid	Perfect
Labyrinth	89	29	17	12
Braid	**94**	52	15	11
Partial Braid	85	**71**	**46**	**36**
Perfect	53	65	44	34
Random	-	-	24	9.5

training against more complex environments.

When comparing path lengths for braid and partial-braid mazes, we selected a maximum number of steps for the random policy. (Had we not, the random policy might never complete when run on braid or partial braid mazes.) We use a maximum number of steps cutoff for which the random policy demonstrated a performance equal to the average performance of all the E2E-RL agents over all maze types.

Table 4 reports path length results for 7x7 mazes and Table 5 reports path length results for 9x9 mazes. For 7x7 mazes on all classes except labyrinth and braid, the policy trained on partial braid and perfect mazes performed best, with the policy trained on perfect mazes performing the best on 9x9 mazes over both braid and partial braid environments. With the exception of the random policy on the labyrinth and braid classes, the policy trained on partial braid mazes was more likely to succeed, especially as 9x9 mazes were considered, yet the policy trained on perfect mazes found the path most quickly.

For the labyrinth and braid mazes, the random policy is guaranteed to find a solution if run for a sufficiently long time as the random policy does not set the turning angle but rather just identifies the next empty block. As it cannot crash the vehicle, and there are no dead ends, eventually it will be successful. For the other policies, the policy does choose the turning angle and thus even for labyrinth and braid mazes, failure of the policy is a possible outcome.

Table 4: E2E-RL average path length for successes on 7x7 mazes over 100 trials. 1 unit = width of a cell. Lower values are better. Best performing policy for each test class is in bold.

Test → Train ↓	Braid	Partial Braid
Labyrinth	16.94	11.83
Braid	14.69	13.31
Partial Braid	**11.85**	11.00
Perfect	11.95	**10.46**
Random	19.59	15.85

Table 5: E2E-RL average path length for successes on 9x9 mazes over 100 trials. 1 unit = width of a cell. Lower values are better. Best performing policy for each test class is in bold.

Test → Train ↓	Braid	Partial Braid
Labyrinth	22.69	16.70
Braid	22.27	20.00
Partial Braid	16.39	14.17
Perfect	**15.14**	**13.63**
Random	27.08	22.98

4.4 Real World Validation

The simulations used above make strong assumptions about the ability of a robot to obtain good odometry and orientation information, and to be able to capture and use simulated LIDAR to obtain state information about obstacles in the environment. In order to validate these assumptions we conducted indoor and outdoor experiments with a wheeled mobile robot. These experiments did not validate end to end performance of the policies developed here, but rather were used to validate the ability of obtaining state information and providing action information to a real robot. For real world experiments, a E2E-RL navigation function trained on braid mazes.

Experiments were performed using an Adept skid-steer P3-AT base augmented with LIDAR, GPS receiver, gyroscope and on board computation. The P3-AT's skid steer was used to simulate Ackermann kinematics. Given the size of the P3-AT, for real world validation the cell size in the maze was set to 2.2m x 2.2m. Space did not permit testing on full 7x7 mazes, as such mazes would require 15m x 15m testing environments and the construction of hundred of meters of temporary walls, so real world experiments were limited to smaller maze structures to explore the ability of the E2E-RL algorithm to navigate complex junctions and corners in the maze. Custom

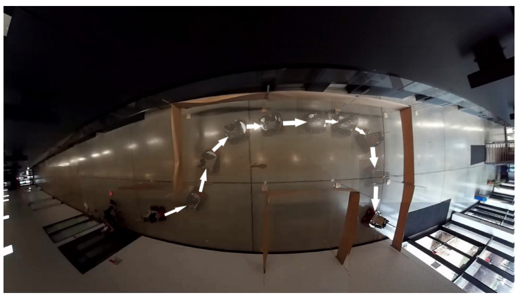
(a) Indoor environment

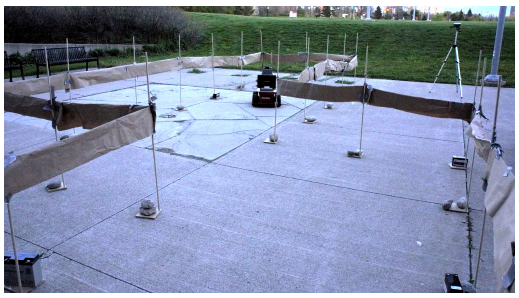
(b) Outdoor environment

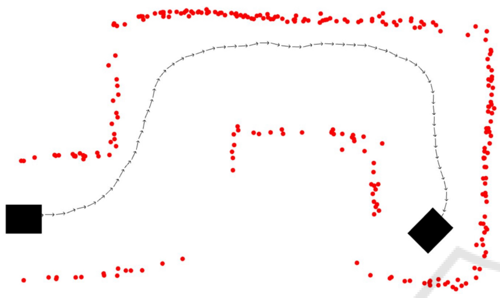
(c) Indoor navigation

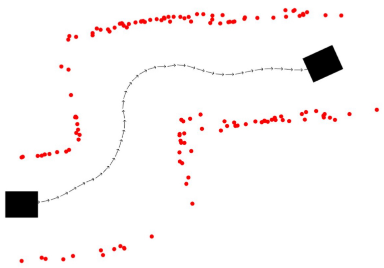
(d) Outdoor navigation

Figure 3: Real world navigation. Indoor and outdoor environments and snapshots of the motion of the robot as recorded by ROS.

ROS nodes were developed to control the robot from an off-robot control station. Uncertain weather conditions required that experiments be conducted both indoors and out. For localization outdoors, a Real-Time Kinematic (RTK) Global Positioning System (GPS) (NovAtel, 2020) was used. For indoor localization, where GPS signals were not available, hand measurements were used as a replacement for the GPS measurement. Although there are more precise automated methods for indoor localization such as WiFi localization (Sun et al., 2014), hand measurement was used here. For orientation information a gyroscope (Passaro et al., 2017) was used to determine orientation and angular velocity. A Phidget Spatial sensor (Phidgets, 2020) was mounted on the robot and data provided to the ROS stack. For obstacle detection, the YDLidar G4 was used. This LIDAR provides denser samples than the nine used in the policies developed here, but the signal was sampled to obtain the nine-dimensional range signal.

4.4.1 Indoor Experiments

Indoor experiments were conducted in the Sherman Health Sciences Building at York University in Toronto, Canada. In order to construct a sufficiently complex environment of the correct scale, existing walls in the building were supplemented with movable wall obstacles that provided a wall like barrier that could be captured by the LIDAR (Figure 3(a)). Given the complexity of estimating vehicle position, indoor experiments were quite time consuming, but these demonstrated that the assumptions that underlie the DRL navigation algorithm applied in this environment. The navigation function was successful for 100% on the three indoor environments constructed. Each test required approximately 12m of robot motion through the maze. Figure 3(c) shows the successful navigation of part of an indoor maze.

4.4.2 Outdoor Validation

Outdoor experiments were conducted on the concrete/stone apron adjacent to the Sherman Health Sciences Building at York University (Figure 3(b)). This apron was sufficiently large to permit a range of different junctions to be modelled and navigated. Four test environments were constructed and the navigation function was successful in navigating all of them. The paper “LIDAR walls” used to construct the environment were impacted by the windy conditions present during the experiments, and the uneven concrete apron around the building impacted vehicle motion and LIDAR angle relative to the ground plane. Although this produced a much more noisy LIDAR signal (visible in Figure 3(d)) and introduced noise into the motion executed by the vehicle, for the four outdoor tests the robot was successful in making its way to the goal location. Each test required approximately 15m of robot motion through the maze.

5 SUMMARY AND FUTURE WORK

Evaluation of end-to-end RL on different environment types with non-holonomic vehicles showed the advantage of training on more complex environments (partial braid and perfect mazes) in terms of both probability of success and the length of the found path to the goal. Validation with real hardware demonstrated that the assumptions made in terms of the E2E-RL formulation were realistic.

ACKNOWLEDGEMENTS

This work was supported by the Natural Sciences and Engineering Research Council (NSERC) through the NSERC Canadian Robotics Network (NCRN).

REFERENCES

Devo, A., Costante, G., and Valigi, P. (2020). Deep reinforcement learning for instruciotn following visual navigation in 3d maze-link environments. *IEEE Robotics and Autonomation Letters*, January.

Dudek, G. and Jenkin, M. (2000). *Computational Principles of Mobile Robotics*. Cambridge University Press, Cambridge, UK.

Faust, A., Ramirez, O., Fiser, M., Oslund, K., Francis, A., Davidson, J., and Tapia, L. (2018). PRM-RL: Long-range robotic navigation tasks by combining reinforcement learning and sampling-based planning. In *IEEE International Conference on Robotics and Automation (ICRA)*, Brisbane, Australia.

Haarnoja, T., Zhou, A., Abbeel, P., and Levine, S. (2018). Soft actor-critic: Off-policy maximum entropy deep reinforcement learning with a stochastic actor. *International Conference on Machine Learning (ICML)*.

Hill, A., Raffin, A., Ernestus, M., Gleave, A., A, K., Traore, R., Dhariwal, P., Hesse, C., Klimov, O., Nichol, A., Plappert, M., Radford, A., Schulman, J., Sidor, S., and Wu, Y. (2018). Stable Baselines. https://github.com/hill-a/stable-baselines.

Karaman, S. and Frazzoli, E. (2011). Sampling-based algorithms for optimal motion planning. *The International Journal of Robotics Research*, 30:846–894.

Lavalle, S. M. (1998). Rapidly-exploring random trees: A new tool for path planning. Computer Science Department, Iowa State University.

Matthews, W. H. (1927). *Mazes and Labyrinths: Their History and Development*. Dover. Dover Publication Reprint, 1970.

Mnih, V., Badia, A. P., Mirza, M., Graves, A., Lillicrap, T. P., Harley, T., Silver, D., and Kavukcuoglu, K. (2016). Asynchronous Methods for Deep Reinforcement Learning. *International Conference on Machine Learning (ICML)*.

Mnih, V., Kavukcuoglu, K., Silver, D., Graves, A., Antonoglou, I., Wierstra, D., and Riedmiller, M. (2013). Playing Atari with deep reinforcement learning. *CoRR*.

NovAtel (2020). Real-time kinematic (rtk). https://novatel.com/an-introduction-to-gnss/chapter-5-resolving-errors/real-time-kinematic-rtk. Accessed: 2020-07-30.

Passaro, V. M. . N., Cuccovillo, A., Vaiani, L., Carlo, M., and Campanella, C. E. (2017). Gyroscope technology and applications: A review in the industrial perspective. *Sensors*, 17(10):2284.

Phidgets (2020). Phidgets spatial user guide. https://www.phidgets.com/. (accessed August 12, 2020).

Pullen, W. D. (2020). Maze classification. https://www.astrolog.org/labyrnth/algrithm.htm. (accessed August 12, 2020).

Schulman, J., Moritz, P., Levine, S., Jordan, M., and Abbeel, P. (2015). High-dimensional continuous control using generalized advantage estimation. *CoRR*.

Silver, D., Huang, A., Maddison., C., Guez, A., Sifre, L., van den Driessche, G., Schrittwieser, J., Antonoglou, I., Panneershelvam, V., Lanctot, M., Dieleman, S., Grewe, D., Nham, J., Kalchbrenner, N., Sutskever, I., Lillicrap, T., Leach, M., Kavukcuoglu, K., Graepel, T., and Hassabis, D. (2016). Mastering the game of Go with deep neural networks and tree search. *Nature*, 529(7587):484–489.

Sun, Y., Liu, M., and Meng, M. Q. (2014). Wifi signal strength-based robot indoor localization. In *IEEE International Conference on Information and Automation (ICIA)*, pages 250–256, Hailar, China.

Tai, L., Paolo, G., and Liu, M. (2017). Virtual-to-real deep reinforcement learning: Continuous control of mobile robots for mapless navigation. In *IEEE/RSJ International Conference on Intelligent Robots and Systems (IROS)*, Vancouver, Canada.

Turidus (2017). Python-Maze. https://github.com/Turidus/Python-Maze.

Wanmg, J., Elfwing, S., and Uchibe, E. (2021). Modular deep reinforcement learning from reward and punishment for robot navigation. *Neural Networks*, 135:115–126.